Europ.J.Hort.Sci., **74** (6). S. 260–267, 2009, ISSN 1611-4426. © Verlag Eugen Ulmer KG, Stuttgart

Modelling Apple Fruit Yield Using Image Analysis for Fruit Colour, Shape and Texture

D. Stajnko[1)], J. Rakun[1)] and M. Blanke[2)]
([1)]University of Maribor, Faculty of Agriculture and Life Sciences and [2)]University of Bonn, INRES – Horticultural Science)

Summary

This work describes a new, computerised vision-based model to estimate the diameter and number of apple fruit on a tree and hence its yield autonomously under natural weather conditions in a fruit orchard. A charge-coupled device (CCD) camera acquired images of cvs 'Golden Delicious' and 'Jonagold' apple (*Malus domestica* L. Borkh.) trees seven times in the vegetation period, i.e. every two weeks from June to September 2007 for modelling the tree volume, fruit diameter and yield at harvest time. Images were processed off-line using image analysis for fruit colour, shape and texture. The fruit detection algorithm was successfully tested on trees bearing from 15 to 42 apple fruits and missed or mis-classified 1 to 3 apple fruits per tree. Fruit detection was sufficiently accurate with an 89 % rate and an overall error rate of 2.2 %. Fruit diameter was underestimated at the beginning of fruit growth in June, but the data corresponded closely ($R^2 = 0.96$) with orchard measurements from July onwards, which enabled accurate modelling of the expected yield per tree. The proposed autonomous model hence has a large potential for forecasting the yield in June/July of harvest in September/October initially of apple in Europe and in the Northern hemisphere.

Key words. apple – image analysis – image processing – modelling – yield prediction

Introduction

In the European Union (EU-25), about 10 million t of apples are harvested every year, but with great fluctuations from year to year and from orchard to orchard. Yield prediction is hence a pre-requisite for all partners in the food chain, orchard owners, trade, shippers and retailers who all require data on fruit quantity at different fruit growth stages, since a tree bearing an excessive number of fruits will yield small, undersized fruits. Thus, modelling fruit growth with an emphasis on tree variability is a crucial step in the management of fruit quantity and quality through horticultural practices (Lescourret et al. 1998) with a great impact on yield prediction per hectare in every growing region. Oriade and Dillon (1997) investigated the variability of fruit growth by using a stochastic approach of fruit growth rates and considering the sink strength of the fruit. However, all these models simulate the environmental conditions in the orchard, which can significantly vary from the real values.

To overcome these disadvantages, Welte (1990) refined the original Bavendorf model (Winter 1979) by introducing orchard measurements in the mechanistic models. However, fruit are still manually counted on the tree in the orchard by visual inspection on a few selected sample trees, which is labour intensive and time consuming, hence leaving this method inappropriate for modelling fruit yield in an individual orchard as required by the fruit industry (Stajnko et al. 2004). The accuracy of these prediction methods can be improved by visual techniques to collect sample data. At present, vision algorithms are used for detecting fruits by harvesting machines in experimental cases restricted to control lighting conditions (Safren et al. 2007). Image processing, as a machine vision tool, provides information e.g. about plant size, population density, plant health or fruit detection (Hemming and Rath 2002).

Fruit detection algorithms automatically process fruit characteristics in artificially lighted environments, but currently new fruit recognition algorithms are developed for orchard conditions e.g. for the detection of ripening apple fruits with an accuracy of 84 % being reported by Sites and Delwiche (1988), 75 % by Slaughter and Harrel (1989), 80 % by Juste and Sevilla (1991), 88 % by Bulanon et al. (2002) and Safren et al. (2007), and 90 % by Stajnko et al. (2004).

Approaches used to detect fruits on trees or on the ground, to count them or to guide robotic arms towards them, can be classified into three groups according to the techniques employed:

The first group of authors relied on the use of range sensors or stereovision systems, as described by Jimenéz et al. (1999) and Benady and Miles (1992). They offer a unique view of the scene, providing range data, which represent measurements of distance from the range sensor to the observed object. Based on range data, the curvature of observed objects can be determined. In case the region in question has the right shape, it is likely to represent the searched

objects. The process gains complexity as scene complexity increases. Furthermore, range sensors represent specialized equipment that is rarely available in the field.

The procedures described by the second group of authors (D'Esnon 1984; Sites and Delwiche 1988) are based on capturing digitalized images while applying additional lighting to the scene. The illumination conditions are selected with care to promote regions of interest and to suppress surrounding light scatter. Some purposed approaches also use night-time conditions, when there is no interference from other light sources. Presented solutions may therefore be awkward and unpractical.

The last group of authors (Juste and Sevilla 1991; Stajnko et el. 2004; Zaho et al. 2005) propose to apply digitalized images taken by a charge-coupled device (CCD) digital camera without any artificial light sources. Images are captured in an uncontrolled environment using everyday photographic equipment. In contrast to solutions from the previous section, the digitalization step is simple, but the detection step presents the scientific challenge.

As an example of the first group, Tanigaki et al. (2008) presented a cherry harvesting robot that works with the help of 3D vision sensor. The sensor is made up of artificial light sources and two digital cameras that enable the robot to estimate the distance between the sensor and the object by using stereovision approach. The robot is able to detect mature cherries that are picked by using 4 degrees of freedom and effectors.

In their similar work, Van Henten et al. (2003) describe a prototype of a robot that is able to pick cucumbers. It also uses stereovision to locate cucumbers, but still faces some problems. For example, it takes at best 53 seconds to detect and harvest a single cucumber, where authors report 74.4 % success rate after several attempts.

Instead of using an artificial light source and a digital camera, which works by capturing images from visible spectrum to detect fruits, a hyperspectral system could be used. It is more common for quality assessment systems as the one from Goméz-Sanchis et al. (2008), but as the computer power increases with time, it will not be long until practical solutions are reached. The problem that hyperspectral systems face is the amount of data that needs to be processed. In order to reduce this quantity of data, classification and regression trees (CART) or linear discriminate analysis is used.

Schumann et al. (2007) suggested an original approach for sampling the citrus yield by image analysis. They use a colour camera mounted on a pole looking down on tree canopies. Furthermore, they sample the whole orchard by taking overlapping images of every canopy and they also apply a monochrome digital camera with near-infrared band pass filters to produce a multispectral imaging system.

Looking further into the last section, fruits can be detected either by using colour, shape or less frequently, by applying textures. In some cases, two of the properties were used in order to detect fruits. According to proposed classification, our presentation falls into the last section. In contrast to other researchers, who used one or two properties, the present approach relies on all three properties colour, shape and texture. The white-balance adjustment was corrected automatically by the camera and to prevent possible alterations of contours lossless setting in the RAW format was set.

The overall objective of our research was to develop a multistage algorithm for detecting the number of fruits on a tree in the natural environment by using segmentation, circular Hough transformation and phase correlation on images of apple trees. The specific objective of this work was to apply the algorithm for modelling apple fruit development, based on images representing green and red-green apples, since the apple fruits and apple leaves have the same light green colour, not only in the earliest stages of fruit growth, but also when they mature.

Material and Methods

Abbreviations

CCD – charge-coupled device; CHT – circular Hough transformation; HSI – hue, saturation, intensity colour space; RGB – red, green, blue colour space.

Orchard lay-out and fruit trees

Twenty, four-year-old apple cvs 'Golden Delicious' and 'Jonagold' trees on M9 were examined in the Gačnik research centre in Slovenia (46° 36' N, 15° 41' E) from June to September 2007. Digital images were taken in the seven sample dates from June 15th to September 14th at 2 week intervals.

Each series of 20 pictures was taken from the sunny side of the trees and another series from the shaded side, both from a 2.0 m distance from a tree at right angle of 90 ° to the tree row. For the size calibration of any objects in the images, a tennis ball with a standard diameter of 65 mm was positioned in each tree at eye height near the tree trunk and images with a resolution of 2,288 × 1,712 pixels taken with a digital camera type Olympus 765UZ.

Each time all fruit on a tree photograph were counted manually. The diameters of ten fruits from these trees were measured with sliding callipers and fruits were weighted on an electronic balance on the same day. Results were later compared with the image model calculations.

Results

Algorithm

The algorithm processing on a randomly selected sample image of the 'Jonagold' series is summarised in Fig. 1.

Firstly, the algorithm starts on the digitalized images (Fig. 2) by separating pixels to identify and differentiate fruit on the tree from the orchard background. The procedure results in binary images, in which the reconstruction of fruits is based on their shape and size.

A segmentation step proceeds by applying two parallel approaches: the first one segments the image using colour properties and the second one employs their texture properties. Then both binary images are joined together as shown in equation (Eq.) 1, so that a final binary image is produced as the union of overlapping regions (including their non-overlapping parts):

$$\begin{aligned} &\text{bin} = \text{bin_c} \cap \text{bin_t}, \\ &x \in \text{bin}, x \in \text{bin_c and } x \in \text{bin_t}, \end{aligned} \quad (1)$$

where x represents the selected region, bin_c the binarised

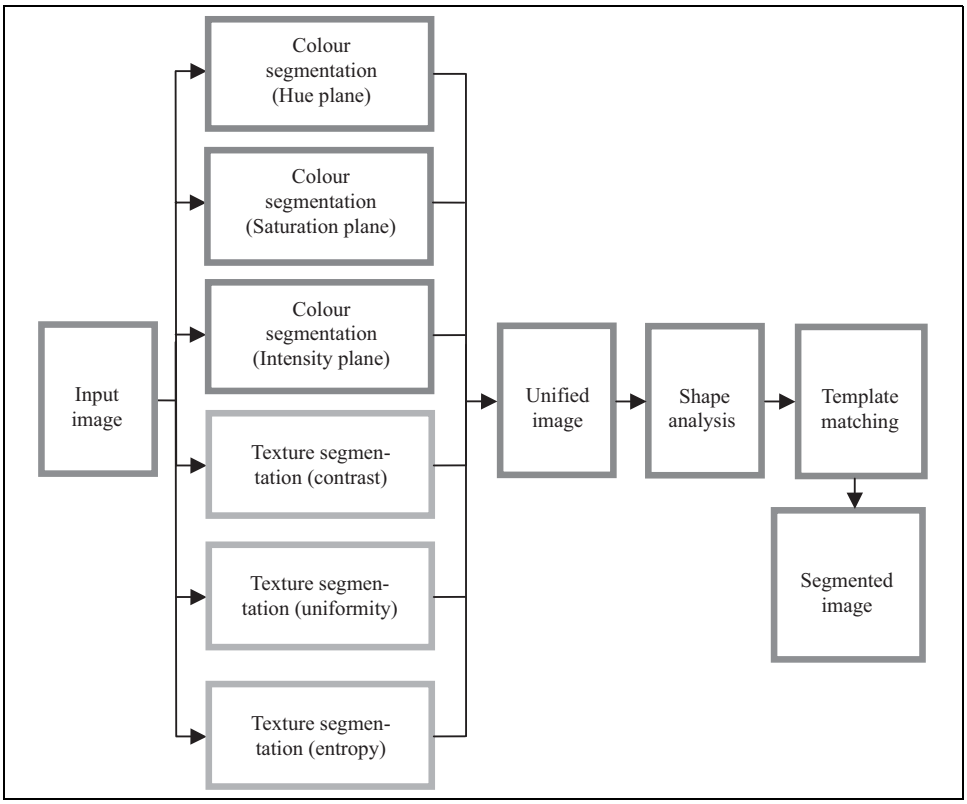


Fig. 1. Flowchart for algorithm to detect apple fruit on the tree in the natural environment of a fruit orchard.

image based on colour segmentation and bin_t the binarised image segmented with the help of texture properties.

Fruits are then reconstructed by applying binary images with the help of a circular Hough transformation (CHT) and correlation measure between template and regions representing fruits.



Fig. 2. Original RGB image of a cv. 'Jonagold' tree at September 14th 2007.

Colour segmentation

In order to segment images on the basis of their colour properties, the HSI colour space with three planes representing hue colour angle, light saturation and light intensity was selected. The HSI colour space is more appropriate for this purpose in contrast to the RGB colour space as it is easier to segment the images based on their hue values. If we focus on hue plane we can omit the influence of sunny and shaded regions that can affect the results. However we must keep in mind that too bright or too dark region can influence the results as the colours tend to obliterate to white or black colour. By looking through our database of shaded and sunny image sets loose empirical thresholds were set (depicted in Table 1). These could be applied to different images representing different fruits, but with correctly selected hue thresholds.

After applying these selected thresholds in the HSI colour space, three intermediary binary results are produced that were later united by using Eq. 2:

$$\text{bin_c} = \text{bin_H} \cap \text{bin_S} \cap \text{bin_I}, \quad (2)$$

where bin_H represents the binary image for hue, bin_S for light saturation and bin_I for the light intensity plane, respectively. Processing an intersection between three partial solutions is based on empirically determined thresholds. Since they are empirical at this stage, some false positive regions were determined, which differ from one partial solution to another one. By applying an intersection to all three binary images, the majority of the false

Table 1. Empirically determined segmentation thresholds. All values are normalised in the range between values 1 and 0.

Plane	Selected values
H (Hue)	[0, 0.1] or [0.9, 1]
S (light saturation)	[0.2, 1]
I (light intensity)	[0.2, 0.8]

positive regions are eliminated. An example of such an intersection is shown in Fig. 3.

However, thresholds cannot be set easily in such a simple way that segmentation alone would include only pixels representing fruits without introducing few unwanted pixels from the background. Therefore, the originally empirically set thresholds (Table 1) should be stricter. A parallel procedure is hence introduced, which grades thresholds images according to their texture properties.

Segmentation using textures properties

As a separate step from colour segmentation, additional segmentation, based on texture properties is done. Based on the work by ZAHO et al. (2005), we applied 24-bit colour images with enhanced texture properties. In the case of images representing mainly red skin cv. 'Jonagold' apples the magnitude of red colour intensities was calculated according to Eq. 3:

$$R_I = 3*R - B - G, \quad (3)$$

where R stands for red, B for blue and G for the green colour plane. Eq. 3 produces an intensity image, which is used to calculate statistical measures for contrast, uniformity and average entropy that correspond to texture properties.

First, average contrast is calculated using Eq. 4:

$$c = 1 - \sum_{i=1}^{K} \sum_{j=0}^{K} (i-j)^2 p_{ij} \quad (4)$$

where p_{ij} represents neighbourhood probability value for selected pixel pair as described by GONZALES and WOODS (2001), K the number of values in one dimension in co-occurrence matrix.

Second, uniformity is calculated by using Eq. 5:

$$U = \sum_{i=0}^{L-1} p^2(z_i) \quad (5)$$

The last texture property used is average entropy shown by Eq. 6:

$$e = -\sum_{i=0}^{L-1} p(z_i) \log_2 p(z_i) \quad (6)$$

As seen in Fig. 4, each texture property produced different results. While areas representing fruits can be clearly identified in each image, all of them were later included in a cumulative result. This was done with the help of superimposing one image on top of another, producing a new intensity image. For final result areas with highest values were looked for, corresponding to top 5 % intensity values.

Shapes and reconstruction – circular shape for fruit

Once a binary image is constructed by Eq. 1, size, number and position of fruits have to be identified. The first step

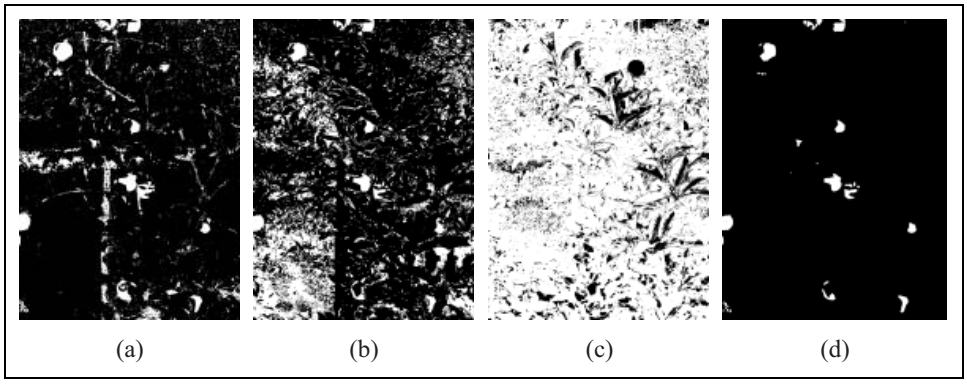


Fig. 3. Images produced by segmentation based on empirically selected colour thresholds representing: segmented hue plane (a), segmented saturation plane (b), segmented intensity plane (c) result of intersection (d) produced by Eq. 2.

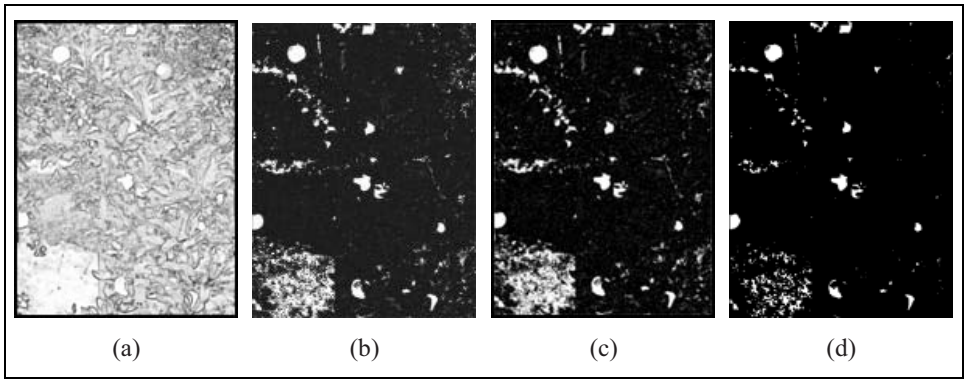


Fig. 4. Images produced by segmentation based on texture properties representing average contrast (a), uniformity (b), entropy (c) and partial binary solution (d).

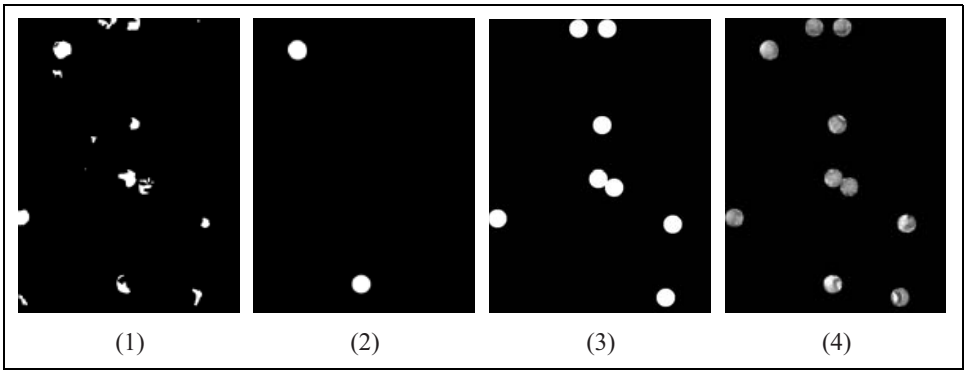


Fig. 5. 1st image represents binary image produced by both segmentation steps, 2nd the result of CHT, 3rd template matching done with the help of phase correlation and 4th the final result.

of this procedure detects (apple) fruit by their circular shapes using CHT, as described by Gonzales and Woods (2001). For undetected regions, a phase correlation technique is applied. In our case, circular regions represent apple fruits, which are detected in the following three steps.

First, we estimate the radius of regions by use of two perpendicular lines moving from upper left to lower right corner of an image. With each step, all regions that were cut by lines are measured and stored. Based on the distances of the edges for the intersected regions histograms are constructed. The radius is calculated as half the diameter retrieved as local minimum between the two most explicit peaks.

In the second step, edge pixels are identified by placing a circle on each centre of the circumference having radius from the previous paragraph. A matrix called accumulator is then calculated, where a cumulative grade is given for each pixel representing the number of pixels from each circumference that fall on a given pixel position. Distinct local maximum values show up in the centres of round regions (Fig. 5a). Once they are detected, their location is used to construct a partial solution. On each location, a binary template is placed representing a circle with a calculated radius.

Only the most prominent circular regions can be detected using CHT. For the remaining regions, template matching is applied using a circular template. The template is created automatically representing a white circle with a diameter from the previous paragraph. A phase correlation (Gonzales and Woods 2001) is selected for the task of template matching, which produces distinct local maximal values. Once again the position of local maximum values is applied to place a template, revealing the second half of the solution.

At the end, both binary images are united with the help of logical and operation. Logical values 1 are finally replaced by colour values from the original image, revealing the final solution as depicted in Fig. 5.

The number and average diameter of fruits on each image serves as an input for modelling the current yield and forecasting the yield at picking date. For calculating the current yield per tree from the sample image the following Eq. 7 is applied:

$$Y_1 = N \cdot a \cdot D^b \quad (7)$$

where Y_t represents the yield per tree, N the number of fruits per tree, D average diameter and a, b constants depending on apple variety.

The yield estimation for the picking date in September/October is based on a transformation function derived by Welte (1990), which allows a direct calculation of the weight from the fruit diameter. He showed that during the fruit growing the relative increase in diameter was proportional to the relative fruit weight increase.

Digitalisation and image analysis were processed on a personal computer (PC) with 1.81 GHz processor and 1.00 GB random access memory (RAM), using Imaq Vision 6.1., Labview 7.1. from National Instruments® and Matlab 7.5 from The MathWorks™. Recorded fruit characteristics and yield per image were stored for statistical analysis using SPSS Package Program version 13.

Numeric results – number of fruits per tree

To validate the proposed fruit detection algorithm, twenty digitalized images were randomly selected from our sunny and shaded database with 'Jonagold' apple trees on the 7th recording date in September on the grounds of the widest range of fruit set from trees bearing from 15 to 42 apple fruits (Table 2). The detection algorithm proved to be successful as it missed or misclassified only 1 to 3 apple fruits per tree, whereby the fruit detection was accurate with an 89 % recognition rate of all selected cases. The bi-coloured 'Jonagold' apple fruit from the dataset had a distinctive top colour with a uniform shape and radius which enabled to simplify our fruit detection algorithm.

A close correlation between detected and manually counted number of fruits was also reported by Kondo et al. (1998) for a strawberry harvester and Kataoka et al. (1999) for apple harvesting. However, in our research a closer correlation was found also for smaller and less coloured fruits. In contrast to these authors, the present procedure involves not only colour and shape, but also fruit texture, which is already detectable in earlier developing stages, is determined using intensity images and enables yield prediction at an earlier growth stage.

In some cases, the number of fruit still deviates considerably from the manual count (Table 2). This addresses occluded regions of the tree, where leaves or branches cover the apple fruit, making their assessment difficult during counting in the orchard, and were therefore discarded as noise. To address this feature, future investigations should capture images from different angles that would disclose most of the occluded regions within a fruit tree.

Estimation of fruit diameter

The average predicted fruit diameters per tree for different developing stages of 'Golden Delicious' apple fruits are shown in Fig. 6 and 'Jonagold' in Fig. 7, respectively.

Table 2. Results of machine vision detection versus counted cv. ' Jonagold' apple fruit on the tree.

Tree	Counted	Detected	Diff.	False detected	Rate (%)
1	42	38	2	1	90
2	26	26	1	1	100
3	17	15	2	0	88
4	29	32	3	3	110
5	18	18	0	0	100
6	18	17	1	0	94
7	17	17	0	0	100
8	15	14	1	0	93
9	16	15	1	0	94
10	21	18	3	0	86
11	25	25	0	0	100
12	38	38	0	0	100
13	24	20	4	1	83
14	34	36	2	2	106
15	40	38	2	0	95
16	39	37	2	1	95
17	24	15	9	2	63
18	42	40	2	2	95
19	31	30	1	0	97
20	35	33	2	1	94

As seen in the 1st and 2nd recording date, the fruit diameters of the image analysis were higher than the actual fruit diameters, while smaller fruit diameters were predicted at all later records during the vegetation period. The reason for this underestimation of young fruitlet diameters lies in the properties of fruit detection algorithm, which is sensitive to the colour variations of the objects. Since those parameters are not distributed equally all over the spherical 2D presentation of the apple fruits on the image, a lower fruit diameter is usually detected not only on the green-red skin of 'Jonagold', but also on the yellow skin 'Golden Delicious' variety.

These results correspond closely with those of STAJNKO et al. (2004), whenever images were captured by a thermal camera; contrary to our experiment without sensitivity to illumination, the thermal camera was sensitive to the heat emitted by the object viz fruit.

Estimation of fruit yield per tree

The yield per tree was estimated in all images by applying Eq. 7. As seen from Fig. 8 and 9, the average estimated yield per tree was slightly underestimated at the 1st and 2nd recording date. At the following 3rd record date, the manual measurements were practical identical with image algorithm. However, at all successive dates the yield was underestimated, when the image processing procedure was applied. The main reason for those deviations can be given to particular equation, because WELTE (1990) himself found out that the fruit diameter corresponds closer to the fruit mass in the later then earlier growing stages.

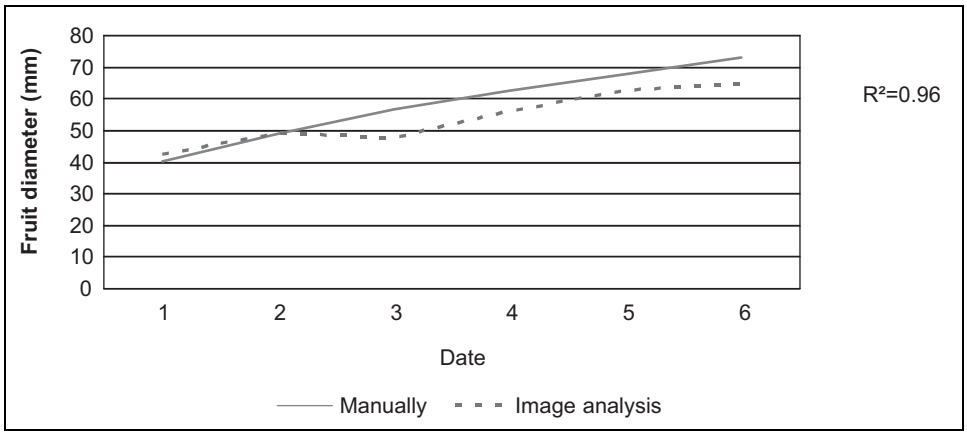


Fig. 6. Comparison between fruit diameter of cv. 'Golden Delicious' apples during fruit ontogeny between manual measurements on the tree in the orchard and image analysis (numbers refer to sampling dates).

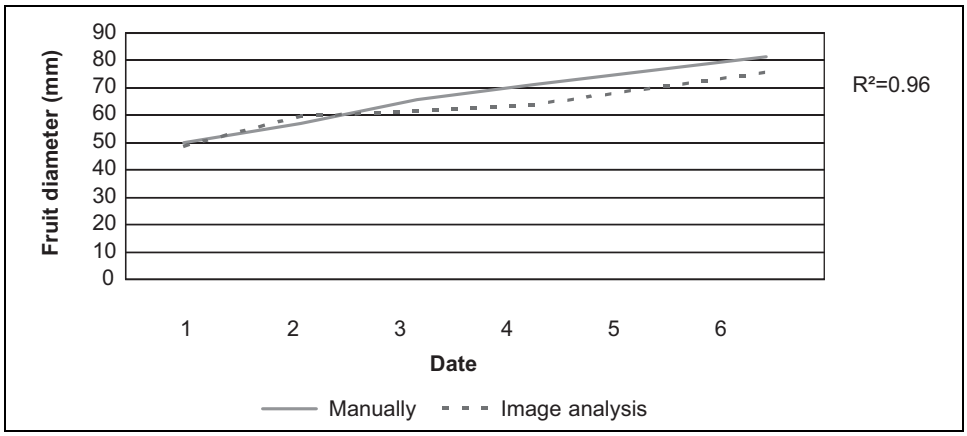


Fig. 7. Comparison between fruit diameter of cv. 'Jonagold' apples during fruit ontogeny between manual measurements on the tree in the orchard and image analysis (numbers refer to sampling dates).

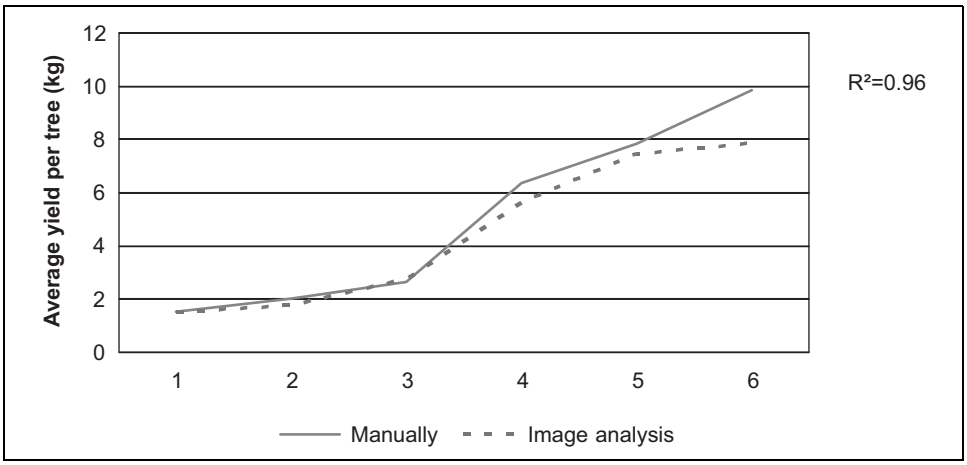


Fig. 8. Comparison between manually measured and modeled tree yields of cv. 'Golden Delicious' apples during fruit ontogeny (numbers refer to sampling dates).

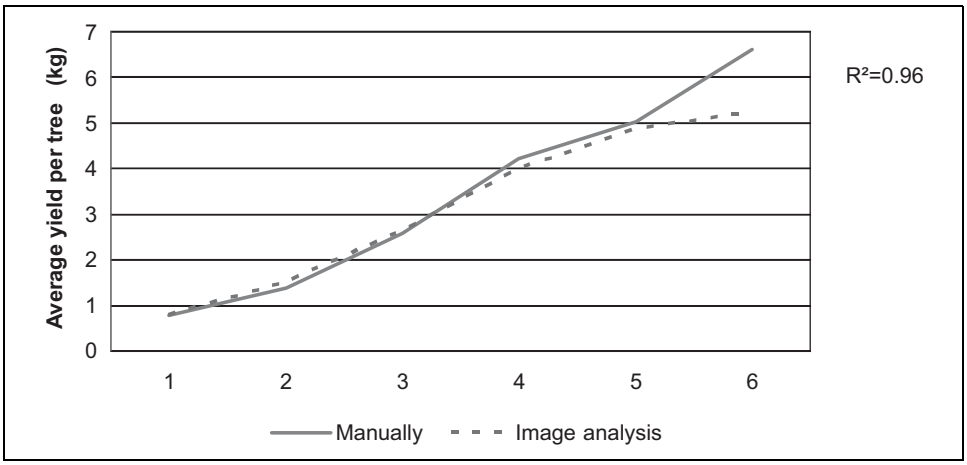


Fig. 9. Comparison between manually measured and modeled tree yields of cv. 'Jonagold' apples during fruit ontogeny (numbers refer to sampling dates).

However, whenever comparing the established growing of fruits developed by the model and manual measurements, almost identical growing curves (R^2=0.96) were estimated for both varieties, which promise a very good possibility of the algorithm for predicting the fruit growth and forecast the harvest date.

The high regression statistics indicate that both models applied in the research estimated the fruit development of 'Golden Delicious' and 'Jonagold' accurately across the whole observing period, although at the 7th date the model slightly underestimated the fruit weight at maturity. The system was proven to facilitate precise, frequent investigation of apple fruits even in the early growing stages when the objects are small and partly hidden in the tree crown, contrary to other authors. However, for extended on-line application in the orchard, the model should be additionally optimised by introducing the algorithm running at two or four multi-core processor.

Processing time

In order to measure the processing time for each step of the algorithm, ten randomly selected images were chosen from our database, having a resolution of 2,288 × 1,712 pixels. For each image the processing time for colour segmentation, texture segmentation, shape analysis and reconstruction was measured separately (Table 3).

The first two steps of colour and texture segmentation required an almost constant time to process one image. On the other hand, the shape analysis and reconstruction prove to be more variable as the processing time differs from one image to another. The reason for this lies in the quality of segmented images and occlusions that may have taken place due to leaves and branches. Thus, in cases where regions on binarised images are already complete after texture and colour segmentation fewer iterations and therefore about 20 seconds less is required to complete the processing, unlike being the way on scattered and smaller incomplete regions.

Conclusion

The proposed model for estimating apple fruit development and yield at harvest, based on colour, shape and texture image analysis, can be employed successfully to provide an easy counting of apples and measurement of their diameters needed for objective modelling of apple development and forecasting yield. In comparison with the current mechanistic models, which are labour intensive due to manual sample counting, it enables faster investigation of larger samples in the orchard and subsequently calculates more accurate forecast.

The system was used successfully during fruit ontogeny between June and September in two different skin colour varieties 'Golden Delicious' and 'Jonagold' in all cases when as little as one third of a round part of the apple was detected. However, the system was not always able to distinguish between fruits and leaves growing

Table 3. Results of measuring the processing time (in seconds) for each of the image processing steps using 10 randomly selected images.

Image	Colour segmentation	Texture segmentation	Shape analysis	Reconstruction
1	10	119	22	10
2	10	119	25	7
3	10	117	3	6
4	10	117	20	12
5	10	117	20	11
6	10	117	21	12
7	10	117	24	11
8	10	117	4	10
9	10	117	21	15
10	10	119	26	11
Average	10	117.6	18.6	10.5
Std. dev.	0	0.97	8.22	2.55

deep in the tree-crown, which can hardly be detected even with a bare eye. Thus, in such cases with clustered regions and less uniform regions, the fruit detection algorithm could be carried out iteratively, revealing fruits of different sizes with each iteration.

Speeding up the processing time can be overcome by implementing more core processors, since the texture calculation currently lasts around 120 s per image and hence a machine vision system could be envisaged for the future for real-time orchard modelling.

The models presented herein can be used to estimate the growing curves of specified varieties 'Golden Delicious' and 'Jonagold' under local conditions but does not allow its direct application to other varieties; however, this forms the basis for further work especially in evaluating particular cases. A slightly lower success rate can be expected for apple varieties with less prominent top colour, clustered regions and less uniform radius. The proposed model hence has a large potential for forecasting the yield at harvest of the entire plantation not only of apple, but also pears whenever additional modifications in algorithm would be introduced.

Acknowledgements

The funding of this research by The Ministry of Agriculture, Forestry and Food of the Republic of Slovenia, project number No. V4-0339-06, is gratefully acknowledged. The author's acknowledge Mr. Storey Lindsay for editing the manuscript.

References

Benady, M. and G.E. Miles 1992: Locating melons for robotic harvesting using structured light, Transaction of the ASAE 92-7021.

Bulanon, D.M., T. Kataoka, Y. Ota and T. Hiroma 2002: A segmentation algorithm for the automatic recognition of 'Fuji' apples at harvest, Biosystems Engin. **83**, 405–412.

D'Esnon, G. 1984: Robot harvesting of apples. Proceedings AgrMation I, 210–214.

Gómez-Sanchis, J., L. Gómez-Chova, N. Aleixos, G. Camps-Valls, C. Montensinos-Herrero, E. Moltó and J. Blasco 2008: Hyperspectral system for early detection of rottenness caused by *Penicillium digitatum* in mandarins. J. Food Engin. **89**, 80–86.

Gonzales, R.C. and R.E. Woods 2001: Digital Image Processing, 2nd Ed.. Upper Saddle River: Prentice Hall PTR.

Hemming, J. and T. Rath 2002: Image processing for plant determination using the Hough transform and clustering methods. Gartenbauwissenschaft **67**, 1–10.

Jimenéz, A.R., R. Ceres and J.L. Pons 1999: A machine vision system using a laser radar applied to robotic fruit harvesting. Proceedings IEEE Workshop: Computer vision beyond the visible spectrum: Methods and applications (CVBVS '99), 110–119.

Juste, F. and F. Sevilla 1991: Citrus: A European project to study the robotic harvesting of oranges. 3rd International Symposium on Fruit, Nut and Vegetable Harvesting Mechanization, 331–338.

Kataoka, T., D.M. Bulanon, T. Hiroma and Y. Ota 1999: Performance of robotic hand for apple harvesting. ASAE St. Joseph, MI-USA, ASAE Paper No. **993003**, 11 p.

Kondo, N., K. Hisaeda and M. Monta 1998: Development of strawberry harvesting robotic hand. ASAE St. Joseph, MI-USA, ASAE Paper No. **983117**, 1–7.

Lescourret, F., M.B. Mimoun and M. Génard 1998: A simulation model of growth at the shoot-bearing fruit level. I. Description and parameterization for peach. Europ. J. Agron. **9**, 173–188.

Oriade, C.A. and C.R. Dillon 1997: Developments and biophysical and bio economic simulation of agricultural systems: a review. Agr. Econ. **17**, 45–48.

Safren, O., V. Alchanatis, V.D. Ostrovsky and O. Levi 2007: Detection of green apples in hyperspectral images of apple tree foliage using machine vision. American Society of Agricultural and Biological Engineers (ASABE): Trans. ASABE **50**: 2303–2313.

Schumann, A.W., K. Hostler, J.C. Melgar and J. Syversten 2007: Georeferenced ground photography of citrus orchards to estimate yield and plant stress for variable rate technology. Proc. Fla. State Hort. Soc. **120**, 56–63.

Sites, P. and M. Delwiche 1988: Computer vision to locate fruit on. A tree. Trans. ASAE, **31**, 257–263.

Slaughter, D. and R.C. Harrel 1987: Colour vision in robotic fruit harvesting. Trans. ASAE **30** 1144–1148.

Stajnko, D., M. Lakota and M. Hočevar 2004: Estimation of number and diameter of apple fruits in an orchard during the growing season by thermal imaging. Comp. and Electr. in Agr. **42**, 31–42.

Stajnko, D. and Z. Čmelik 2005: Modelling of apple fruit growth by application of image analysis. Agric. conspec. Sci. **70**(2), 59–64.

Tanigaki, K., T. Fujiura, A. Akase and J. Imagawa 2008: Cherry-harvesting robot, Comp. and Electr. in Agr. **63**, 65–72.

Van Henten, E.J., B.A.J. Van Tuijl, J. Hemming, J.G. Kornet, J. Bontsema and E.A. Van Os 2003: Field test of an autonomous cucumber picking robot. Biosystems Engin. **86**, 305–313.

Welte, H.F. 1990: Forecasting harvest fruit size during the growing season. Acta Hort. **276**, 275–282.

Winter, F. 1979: Frupro1, a dynamical model connecting biological and economic elements of orchard management. Acta Hort, **97**, 423–425.

Zaho, J., J. Tow and J. Katupitiya 2005: on-tree fruit recognition using texture properties and color data. Conference on Intelligent Robots and Systems, Edmonton, Alberta, Canada, 263–268.

Received: January 16, 2009 / Accepted July 09, 2009

Addresses of authors: Denis Stajnko, University of Maribor, Faculty of Agriculture and Life Sciences, Vrbanska 30, SL-2000 Maribor, Slovenia, and Michael M. Blanke, University of Bonn, INRES – Horticultural Science, Auf dem Hügel 6, D-53121 Bonn, Germany, email: denis.stajnko@uni-mb.si and MMBLANKE@uni-bonn.de.